

# International Journal of Nanoelectronics and Materials

IJNeaM -

ISSN 1985-5761 | E-ISSN 2232-1535



# Enhanced InGaAs/AlAs RTD quantum device with frequency multiplier application

Wan Nurnabilah Zaharim <sup>a</sup>, Mohamed Fauzi Packeer Mohamed <sup>a</sup>, Asrulnizam Abd Manaf <sup>b</sup>, Mohamad Khairi Ishak <sup>c</sup>, Ng Sha Shiong <sup>d</sup>, Muhammad Zeshan Ali <sup>e</sup>, Shahrir Rizal Kasjoo <sup>f</sup>, Mohamad Adzhar Md Zawawi <sup>ag \*</sup>, and Siti Fatimah Abd Rahman <sup>a \*</sup>

- <sup>a</sup>School of Electrical and Electronic Engineering, Engineering Campus, Universiti Sains Malaysia, 14300 Nibong Tebal, Pulau Pinang, Malaysia
- <sup>b</sup>Collaborative Microelectronic Design Excellence Centre (CEDEC), Universiti Sains Malaysia, 11900 Bayan Lepas, Pulau Pinang, Malaysia <sup>c</sup>Department of Electrical and Computer Engineering, Ajman University, Ajman, United Arab Emirates
- dInstitute of Nano Optoelectronics Research and Technology (INOR), Universiti Sains Malaysia, Penang 11800, Malaysia
- Department of Materials, School of Engineering and Technology, National Textile University, 37610, Faisalabad, Pakistan
- Faculty of Electronic Engineering and Technology, Universiti Malaysia Perlis, 02600 Arau, Perlis, Malaysia
- <sup>9</sup>Applied College, Princess Nourah bint Abdulrahman University, Riyadh 11671, Saudi Arabia
- \*Corresponding author. e-mail: adzhar@usm.my (M.A.M.Z) and fatimahrahman@usm.my (S.F.A.R)

Received 2 June 2024, Revised 4 February 2025, Accepted 7 March 2025

#### ABSTRACT

This study presents the development of advanced resonant tunneling diodes (RTD) based on InGaAs/AlAs that have an impressive 80% indium content in the quantum well. These cutting-edge diodes were meticulously grown in-house using the precise technique of molecular beam epitaxy. The proposed RTD showcased remarkable negative-differential resistance characteristics, achieving a  $41 \times 10^3 \, \text{cm}^{-2}$  peak current density (Jp) at  $308 \times 10^{-3} \, \text{V}$ , and a peak-to-valley current ratio of 8.5. A large-signal model of the fabricated RTD was developed in LTspice using experimental current-voltage (I-V) data, enabling the simulation of an RTD-based frequency multiplier circuit. A frequency multiplier with a multiplication factor of three (x3) was created and tested by arranging two RTDs in series to introduce non-linearity in the circuit. The experiment successfully demonstrated a threefold increase in frequency, converting an input signal of 166 MHz (3.07 mW) to an output frequency of 500 MHz (51.57  $\mu$ W). The results highlighted the potential of InGaAs/AlAs RTDs for cost-effective ultra-high-frequency applications, particularly for communication systems, radar, and signal processing.

**Keywords:** Quantum device, Frequency multiplier, Resonant tunneling diode

# 1. INTRODUCTION

Communication circuits, particularly frequency multipliers, have been extensively utilized for generating high-frequency signals in the micro- and millimeter wave spectrum. Multipliers based on complementary-metal-oxide semiconductors, heterojunction bipolar transistors, Schottky diodes, and varactor diodes are known technologies employed in the development of frequency multiplier circuitries [1–4]. Nonetheless, these technologies are complex and seem to necessitate several components to construct a fundamental circuit.

However, RTD now holds the record as the fastest electron device. Researchers have used RTDs with group III–V compound semiconductors extensively due to their exceptional electronic properties that enable high-frequency operations [5]. Typically, two slender barriers enclose a quantum well in the center of this device. A heavily doped semiconductor seals the two ends together to ensure efficient ohmic electrical contact. RTD-based circuits are valuable in various fields, including security, military, medical imaging, astronomy, and ultra-high frequency electronics.

Quantum mechanics, characterized by particles exhibiting wave-like characteristics and movement in wave patterns, constitutes the cornerstone of RTD. In physics, a particle may just surmount a potential barrier if its kinetic energy exceeds the height of the barrier. Meanwhile, for quantum mechanics, a particle with incoming energy exceeding the height of the barrier may pass through it and emerge on the opposite side with a certain probability, provided that the barrier is sufficiently thin and finite.

Advanced Indium Gallium Arsenide (InGaAs)/Aluminum Arsenide (AlAs) epilayers were successfully grown in this study using an in-house molecular beam epitaxy (MBE) approach. Two layers of thin AlAs barriers sandwiched the indium-rich (80%) InGaAs quantum well, as depicted in Figure 1. The differences in bandgap energy between these two materials were exploited to optimize the production of negative differential resistance (NDR). These high-quality epilayers formed the basis for the resonant tunneling diodes (RTDs) demonstrated in this paper.

The hypothesis proposes leveraging advanced materials, such as III-V compound semiconductors like InGaAs, to

enhance quantum tunneling efficiency, given their superior electron mobility of approximately 10000 to 12000 cm²/V.s and compositionally defined energy band structures. The very narrow band gap (0.5 eV) of  $In_{0.8}Ga_{0.2}As$  sandwiched between large band gaps (2.16 eV) of AlAs lowers the first resonance level in the quantum well. As a result, an electron tunnels through the resonance with reduced voltage.

Furthermore, strain engineering, achieved by incorporating highly strained (compressive) pseudomorphic quantum wells within (tensile) strained AlAs, is suggested to optimize electronic band alignment, further boosting tunneling probability, leading to highly efficient electronic devices. To ensure ultra-smooth interfaces and precise layer control, fabrication techniques like molecular beam epitaxy (MBE) are employed, reducing scattering and energy losses.

Additionally, optimizing the thickness and quality of barrier layers is critical to minimizing leakage currents and enabling low peak voltage operation. By tailoring the barrier heights and well depths, the hypothesis also aims to achieve a sharp negative differential resistance (NDR) region with a high peak-to-valley current ratio (PVCR), essential for high-frequency and low-power applications. Ultimately, integrating these advancements is expected to enhance device stability, reproducibility, and overall performance, enabling RTDs to meet the demands of advanced electronic communication systems.

A test application was created to assess how these RTDs perform, using a frequency multiplier circuit. There is an unexplored theoretical study of built-in models for RTDs in SPICE-based simulators, such as LTspice® by Linear Technology. Thus, utilizing the table method is the most straightforward approach to designing and integrating an RTD huge signal model in LTspice. This method requires data points to construct the corresponding current-voltage (I-V) curve. In this work, the I-V characteristic data points were taken from experimental data to ensure the validity of the model, which was then used to simulate and optimize the frequency multiplier circuit.

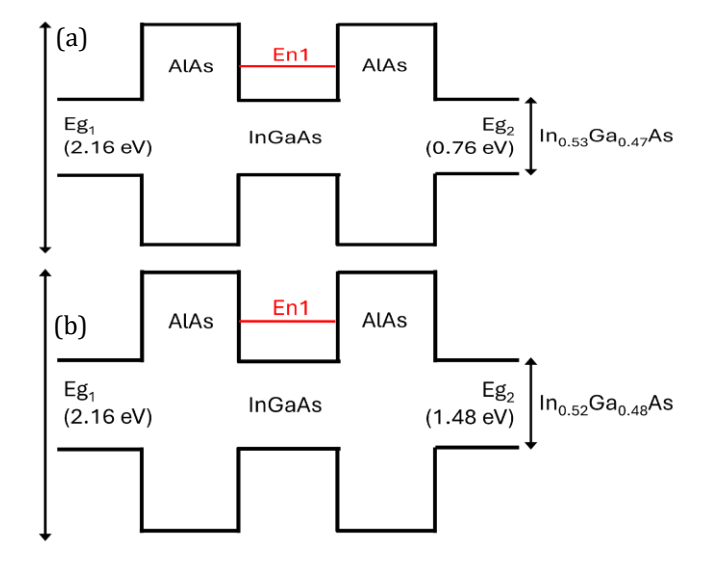


**Figure 1**. Conceptual band diagram of a quantum well with a narrow band gap for (a)  $In_{0.53}$   $Ga_{0.47}$ As and (b)  $In_{0.52}$   $Ga_{0.48}$ As.

# 2. EXPERIMENTAL AND MODELING

#### 2.1. Structures of RTD

The experimental work of RTD was initially conducted by Chang et al. [6]. The authors are concerned about the fundamental configuration of RTD and its commonly seen structures, as outlined by Ling [7]. The utilization of InGaAs/AlAs RTD in this context is one of the limited numbers of indium-rich quantum well structures that have been created using molecular beam epitaxy (MBE). The internally developed and analyzed RTD structure, which is similar to our earlier research [8][9], is summarized in Table 1.

In a double-barrier quantum well (DBQW) system, the confinement of electron and hole motions in the active quantum well area is achieved by sandwiching a layer of narrow bandgap semiconductor between two thin layers of wider bandgap semiconductor in the crystal growth direction. Nonetheless, electrons and holes are capable of unrestricted movement in the opposite direction of growth. The DBQW layers are sufficiently thin compared to the de Broglie wavelength (or electron mean free path). Consequently, the quantum well generates various levels of energy, also known as quantized energy, for electrons and holes. Hence, quantum mechanics, specifically quantum tunneling, primarily governs the electron transport mechanism.

It is worth noting that the total thickness of the double-barrier quantum well structure (DBQW), measuring 6.9 nm, is significantly smaller than the de Broglie wavelength, which typically ranges from 20 nm to 40 nm. While the DBQW thickness is one order of magnitude lower than the de Broglie wavelength, this suggests that the electron tunneling is influenced more by the wavelength of the electron than the well's physical dimensions. The electron's wavelength can span across the entire DBQW, leading to resonant tunneling phenomena and defining the device's electronic properties.

The quantized energy is known to be inversely proportional to the quantum well's thickness. As the thickness of the quantum well diminishes, the quantized energy will rise. The peak voltage and peak current density will rise with the increment of quantization energy. The increased quantization energy necessitates a greater bias voltage to achieve its maximum, resulting in a higher peak voltage. The peak voltage happens when the quantization energy within the quantum well aligns with the conduction band offset. Consequently, RTD performance will improve with the implementation of reduced quantum well thickness.

In addition to quantum well thickness, the effective mass of electrons also influences the quantization energy of the quantum well. It is noted that the effective mass is inversely correlated to the quantization energy. The RTD peak current will rise as the thickness of the quantum well reduces. The barrier thickness, conversely, is a parameter that may be evaluated to achieve optimal performance of the RTD. Employing a quantum mechanical perspective is

essential for comprehending the relationship between current density and barrier thickness,  $t_{\text{\scriptsize b}}.$ 

Layer	Material type	Doping Concentration (cm <sup>-3</sup> )	Thickness (nm)
Collector_A	In <sub>0.53</sub> Ga <sub>0.47</sub> As(n++)	2 x 10 <sup>19</sup>	45.0
Collector_B	In <sub>0.53</sub> Ga <sub>0.47</sub> As(n+)	3 x 10 <sup>18</sup>	25.0
Spacer	In <sub>0.53</sub> Ga <sub>0.47</sub> As	0	20.0
Barrier	AlAs	0	1.2
Quantum Well	In <sub>0.8</sub> _Ga <sub>0.2</sub> _As	0	4.5
Barrier	AlAs	0	1.2
Spacer	In <sub>0.53</sub> Ga <sub>0.47</sub> As	0	4.5
Emitter_A	$In_{0.53}Ga_{0.47}As(n^{+})$	$3 \times 10^{18}$	25.0
Emitter_B	In <sub>0.53</sub> Ga <sub>0.47</sub> As(n+)	1 x 10 <sup>19</sup>	400
Substrate	InP	nil	nil

**Table 1.** InGaAs/AlAs RTD grown in-house by MBE system

The resonant tunnelling current in a double-barrier quantum well structure is contingent upon the transmission probability, *T*, and the wave vector inside the barrier, *K*, as shown in Equations 1 and 2:

$$T\alpha e^{-2Kt_b} \tag{1}$$

$$K = \sqrt{\left(\frac{2m_b v}{h^2}\right)} \tag{2}$$

where  $m_b$  represents the electron effective mass in the barrier and V represents the potential barrier. As the thickness of the barrier decreases, the transmission probability, T, and current density rise exponentially.

The inclusion of the undoped spacer serves to inhibit the diffusion of dopants into the succeeding layer during development. The electron indicates that the free path is unobstructed by ionized donors due to the existence of an un-doped spacer. The presence of an un-doped spacer layer between the contacts, under significant applied bias, facilitates the creation of an initial triangular well, which enhances the resonant tunnelling between the quasi-bound state electron and the resonant state in the quantum well, hence improving the peak-to-valley current ratio (PVCR).

The development of RTDs in this work was adapted from our previously published method [10]. In brief, a conventional i-line optical photolithography technique and wet chemical etching were used to create a mesa of 6  $\mu m^2$  for this two-terminal vertical device. The ohmic contacts were fabricated by thermal evaporation of TiAu for both the emitter and collector to establish electrical contacts for DC measurement.

Nonetheless, other material systems are employed to fabricate RTDs, enhancing the DC properties, such as the peak current density, peak voltage, peak-to-valley current ratio (PVCR), and negative differential resistance (NDR). Diverse material systems will yield varying bandgaps in RTD devices. Consequently, the performance of the RTD device will be impacted by its high speed and complexity. The objective in RTD material engineering is to generate THz RTD application circuits utilizing specialized quantum well structures and to achieve the maximum peak current density.

# 2.2. DC Characteristics

As initially explained by Tsu and Esaki back in 1973 [11], a negative differential resistance (NDR) phenomenon arises in the DBQW structure due to the tunneling effect in nanoscale semiconductors. The experimental values for current–voltage (IV) relations were adapted from the double-barrier resonant tunneling diode (DBRTD) grown, as previously stated [12].

Figure 2 illustrates the IV relations of the RTD. The essential electrical parameters are valley current (IV), peak current (IP), valley voltage (VV), peak voltage (VP), and peak-to-valley current ratio (PVCR). These parameters regulate the power, frequency, and speed capabilities of RTD-based circuits. NDR begins with the peak current and concludes with the valley current. The area will induce negative resistance as it contravenes Ohm's law. PVCR is essential in affecting the NDR. A higher PVCR value corresponds to an expanded NDR area. To achieve a substantial PVCR, the peak current, I<sub>P</sub>, should be maximized, but the valley current, I<sub>V</sub>, should be minimized.

Nevertheless, an excessively large peak current,  $I_p$ , may be impractical because of the problem of high-power dissipation, as elevated peak voltage results in increased power dissipation. This issue can be addressed by engineering an RTD with a very low peak voltage,  $V_p$ , in this study.

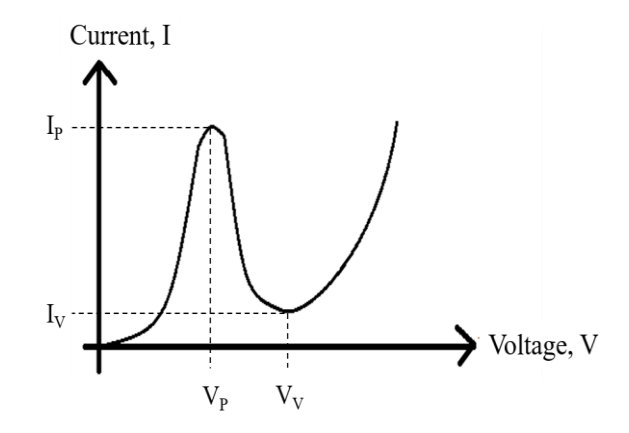


**Figure 2**. Current-voltage relations of DBRTD with negative differential resistance.

DC measurements at room temperature were conducted by using an HP4142B parameter analyzer. This unipolar device (both are of n-type electrodes) manifested a clear negative-differential-resistance (NDR) characteristic as shown in Figure 4 in the next section. It is worth noting that a minimum plateau region within the NDR is observed in real measurement due to DC bias-related small frequency oscillation.

# 2.3. LTspice Modelling

The LTspice table approach utilizes a sequence of measured voltages and currents to precisely define a transfer function. This work used data points from the actual measurement and characterization of the RTD device, obtained through experimental work. Henceforth, the IV curve obtained was accurate and authentic when compared to alternative techniques like equations and polynomial fits, which cover the plateau area inside the NDR zone. The measured value was made of pairs of voltage and currents that showed how these two elements relate to each other, so that the intended IV curve of any RTD devices can be simulated.

The SPICE large signal model for RTD [13] depicted in Figure 3(a) was examined and utilized in LTspice to simulate the main signal characteristics of the device. Before proceeding, it was necessary to calculate the values of internal capacitance ( $C_{rtd}$ ) and series resistance (Rs) using Equations (3) and (4), accordingly [14].

$$C_{\rm rtd} = \varepsilon_0 \varepsilon_{\rm r} A / d \tag{3}$$

$$Rs = R_o/A_{rtd}$$
 (4)

where,  $\epsilon_0$ = 8.854 × 10<sup>-12</sup> F/m,  $\epsilon_r$ = 13.9 (In<sub>0.53</sub>Ga<sub>0.47</sub>As permittivity constant), 13.1 (GaAs permittivity constant), A<sub>rtd</sub>= 6  $\mu$ m × 6  $\mu$ m, d=Quantum Well Thickness + (2 Barrier Thickness) + Spacer<sub>1</sub> Thickness + Spacer<sub>2</sub> Thickness, and R<sub>0</sub>≈ 54  $\Omega/\mu$ m<sup>2</sup> (parasitic structure resistance).

From Equations (3) and (4), d and  $A_{rtd}$  represent the distance of RTD from the first spacer to the second spacer, and the areas of the RTD device, respectively.  $R_s$  represents the contact resistance or contact loss since the device is not ideal for this research, and  $R_o$  represents the resistance of the parasitic layer structure that inherently exists in this device. As evident, the quantum well thickness and barrier thickness values for the InGaAs/AlAs RTD were 4.5 nm and 1.2 nm, respectively. The spacer<sub>1</sub> and spacer<sub>2</sub> thicknesses were 20 nm and 4.5 nm, respectively. Therefore, the distance was calculated as 31.4 nm.

After determining the values of passive components such as resistors and capacitors, the voltage-controlled current source (VCCS) played a significant role in simulating the IV characteristics of RTD. Subsequently, a component symbol depicting an RTD, as seen in Figure 3(b), was generated in the LTspice library, resembling the existing components like resistors, transistors, capacitors, and so on.

The frequency multiplier circuit featured in this work, as shown in Figure 4, is similar to the one suggested by Nafea and Dessouki [15]. To achieve multipeak characteristics,

this RTD-based communication circuit merely comprises two series-connected RTDs as the active devices with a load resistor, R1 (passive device). An optional DC-bias (V1) is included for an initial selection of the operating point for this non-linear circuit. Evidently, this three-component circuit emphasized the reduced complexity of the frequency multiplier circuit.

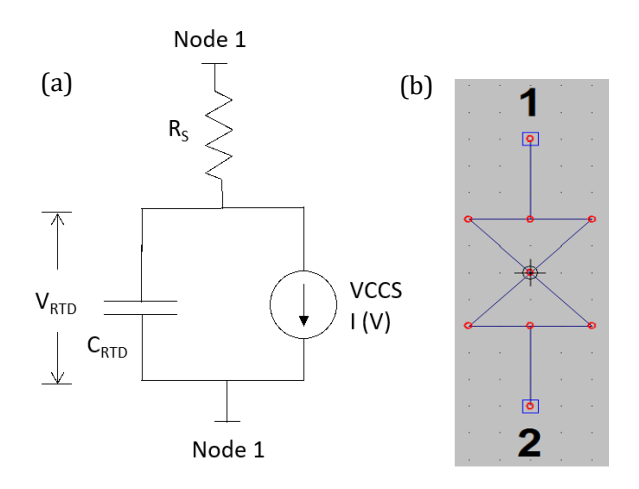


**Figure 3**. (a) Generic SPICE large signal model of a resonant tunneling diode [13] and (b) the component symbol for a double-barrier InGaAs/AlAs resonant tunneling diode developed using LTspice.

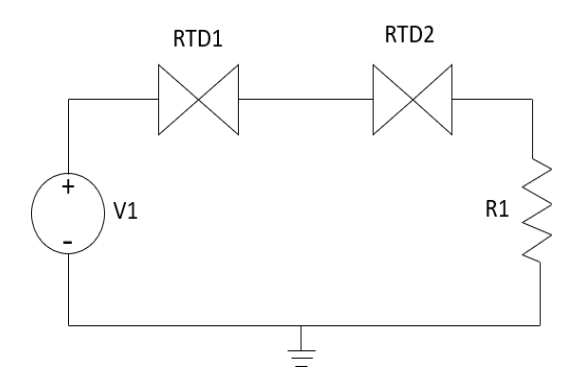


**Figure 4**. Frequency multiplier circuit based on an InGaAs/AlAs resonant tunneling diode for this study.

# 3. RESULTS AND DISCUSSIONS

# 3.1. Model of Large Signal

Table 2 represents a comparison between the computed and simulated values for the  $C_{rtd}$  and Rs parameters. The measured Rs value was lower (0.1  $\Omega$ ) compared to the calculated value (1.5  $\Omega$ ) since a higher series resistance was expected during the fabrication of the real device. The slight discrepancy in series resistance can be attributed to parasitic elements and contact resistances in the actual device, which were minimized in the simulation environment.

Figure 5 displays the reliable RTD IV characteristics for both modeled and experimental data. An observed peak current (IP) of 14 mA was recorded at 308 mV, while a valley current (VV) of 1.65 mA was measured at approximately 700 mV. The peak-to-valley current ratio (PVCR) obtained was 8.48. These values indicate a highly efficient electron

tunneling process, which is essential for high-frequency applications [16]. The way the NDR behaved matches the way quantum tunneling works in double-barrier quantum

well (DBQW) structures, which was originally explained by Tsu and Esaki [10].

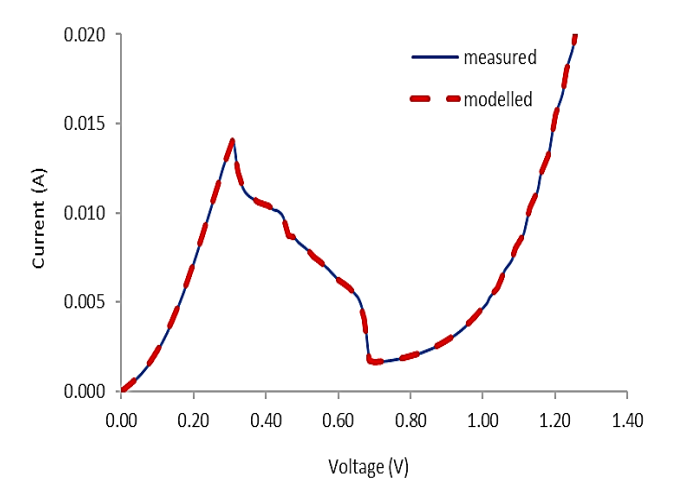
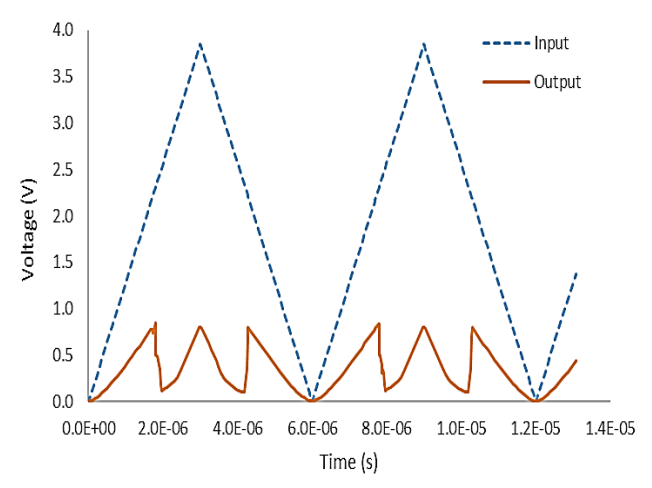


Figure 5. IV characteristics of the InGaAs/AlAs RTD with 6  $\mu$ m<sup>2</sup> mesa area for both modelled and experimental showed excellent fitting



**Figure 6.** RTD-based times three (x3) frequency multiplier sawtooth input and output waveforms from LT-spice (output signal tapped across resistor R1).

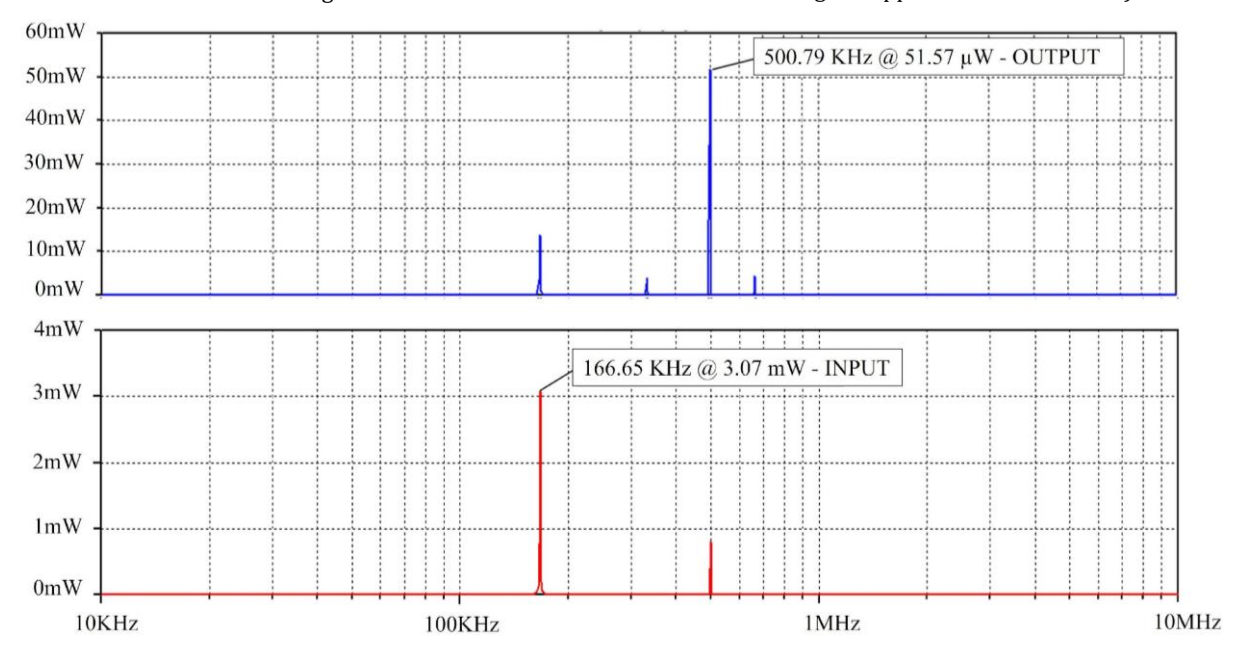


Figure 7. Simulated frequency and power for the RTD-based times three (x3) frequency multiplier.

The experiment and simulation results from the InGaAs/AlAs resonant tunneling diodes (RTDs) highlight several significant findings and potential applications in high-frequency electronics. The RTD with an indium-rich (80%) In $_{0.8}$ Ga $_{0.2}$ As quantum well was successfully fabricated and characterized. This shows that in-house molecular beam epitaxy (MBE) can produce high-quality, highly strained quantum well structures.

# 3.2. Frequency Multiplier

Frequency multiplication may be accomplished by employing a suitable input voltage level. To generate a sawtooth waveform, changes must be made to the LTspice settings for the pulse function, current, output resistor, and transient parameters, considering the individual characteristics of the RTDs. The simulation utilized a pulse

function (V1) with a voltage ( $V_{on}$ ) of 3.85 V. The period ( $T_{period}$ ) was established at 6  $\mu$ s, corresponding to an input frequency of 166 MHz. Furthermore, both the rising time ( $T_{rise}$ ) and falling time ( $T_{fall}$ ) were established at 3  $\mu$ s.

The value of the output resistance (R1) was set to 20  $\Omega$ , which is sufficient to stabilize the modest direct-current (DC) bias oscillation within the RTDs. The  $V_{on}$  value was changed to 3.85 V to achieve a comparable peak of the output waveform at a frequency of around 500 MHz. This frequency is thrice the input frequency and is frequently employed in cognitive radio applications. To commence the creation of a sharp-peak sawtooth waveform, the voltage-controlled current source (VCCS) parameters should be configured to -1.50 V for voltage and -35.5 mA for current. This is essential due to the non-ideal nature of the RTD big signal model. The resultant waveform is seen in Figure 6.

When it comes to power performance, Figure 7 shows that the successfully simulated times-three (x3) frequency multiplier had an output power of 51.57  $\mu$ W (-12.88 dBm) for an input power of 3.07 mW (4.87 dBm). The resulting output power was lower than the theoretical maximum RF

output power of the RTD, which is approximately 1.4 mW (for  $6\times 6~\mu m^2$  mesa), potentially due to loss via the resistor. Thus, optimization of circuit elements, such as reducing resistive losses, could enhance performance further.

**Table 2.** Resistance and capacitance values.

Device Parameter	Resistance (Ω)	Capacitance (pF)
Calculated value	1.500	0.141
Modelled value	0.100	0.141

Figure 6's output, displaying a sawtooth waveform, validates the non-linear operation necessary for frequency multiplication. The ability to achieve frequency multiplication with a simple circuit configuration, comprising only two RTDs and a load resistor, highlights the potential for reduced complexity in high-frequency circuit designs. This suggests great potential for future high RF-power-density operation. Other than that, the frequency multiplier at higher speeds also shows the conduct of multi-valued logic (MVL), for which the exhibited logic state was greater than two. Hence, investigating the scalability of these devices for integration into larger, more complex circuits and systems, including MVL applications, is of great interest as well.

Furthermore, in comparison to conventional multipliers utilizing Schottky diodes [18, 19] and GaAs-based resonant tunneling diodes [20, 21], this study demonstrates lower input power, improved voltage stability, and the capability of enduring the highest output voltage peak-to-peak,  $V_{\rm pp}$ . Notably, the proposed method offered the best efficiency of 2% with respect to the recent findings reported by Zhang and group [22], thereby indicating its suitability for low-power applications.

# 4. CONCLUSION

A highly strained (compressive) indium-rich (80%) quantum well was successfully fabricated characterized in an InGaAs/AlAs resonant tunnelling diode. The PVCR of 8.5 demonstrated a significant peak current density, namely J<sub>P</sub> of 41 kA/cm<sup>2</sup> at 308 mV. A highperformance RTD model incorporating an exceptional material system was successfully shown using LTspice. The model accurately matched the observed values. The outcome of the functional times-three frequency multiplier complexity with reduced showed the possible implementation of RTD integration into economical highspeed and extremely high-frequency circuits for applications in communications, radar, and signal processing.

# **ACKNOWLEDGMENTS**

This work was financially supported by Fundamental Research Grant Scheme from Ministry of Higher Education Malaysia (FRGS/1/2022/TK0/USM/02/10) and Universiti Sains Malaysia (RUI Grant: 1001/PELECT/8014048).

# REFERENCES

- [1] H. Xu, J. Yang, C. Zhuo, T. Kämpfe, K. Ni and X. Yin, "Reconfigurable Frequency Multipliers Based on Complementary Ferroelectric Transistors," 2024 Design, Automation & Test in Europe Conference & Exhibition, Valencia, Spain, 2024, pp. 1-6.
- [2] Z. Liu and F. Liu, "Design of a planar frequency doubler with schottky diodes at terahertz band", 2022 International Conference on Microwave and Millimeter Wave Technology (ICMMT), pp. 1-3, 2022.
- [3] Jeong, Jinho, Jisu Choi, Jongyoun Kim, and Wonseok Choe, "H-Band InP HBT Frequency Tripler Using the Triple-Push Technique" Electronics 9, no. 12: 2081, 2020.
- [4] Zhang, Yong, Chengkai Wu, Xiaoyu Liu, Li Wang, Chunyue Dai, Jianhang Cui, Yukun Li, and Nicholas Kinar, "The Development of Frequency Multipliers for Terahertz Remote Sensing System" Remote Sensing 14, no. 10: 2486, 2022.
- [5] J. P. Sun, G. I. Haddad, P. Mazumder, and J. N. Schulman, "Resonant tunneling diodes: models and properties," *Proceedings of the IEEE*, Vol. 86, No. 4, pp. 641-660, April 1998, doi: 10.1109/5.663541.
- [6] L.L. Chang, L. Esaki, and R. Tsu, "Resonant Tunneling in Semiconductor Double Barriers", *Applied Physics Letters*, Vol. 24, Issue 12, pp. 593-595, 1974, doi: doi.org/10.1063/1.1655067.
- [7] J. Ling, "Resonant tunneling diodes: Theory of operation and applications", University of Roschester, Roschester, New York, Vol. 14627, 1998.
- [8] M.A. Md Zawawi, KaWa Ian, J. Sexton and M. Missous, "Fabrication of Sub-micrometer InGaAs/AlAs Resonant Tunneling Diode Using a Tri-layer Soft Reflow Technique with Excellent Scalability", IEEE Transactions on Electron Devices, 2014.
- [9] S. G. Muttlak, O. S. Abdulwahid, J. Sexton, M. J. Kelly and M. Missous, "InGaAs/AlAs Resonant Tunneling Diodes for THz Applications: An Experimental Investigation," in *IEEE Journal of the Electron Devices* Society, vol. 6, pp. 254-262, 2018.
- [10] Mohamad Adzhar Md Zawawi and Mohamed Missous, "Design and Fabrication of Low Power GaAs/AlAs Resonant Tunneling Diodes", Solid-state Electronics, 2017
- [11] R. Tsu, and L. Esaki, "Tunneling in a finite superlattice," *Applied Physics Letters*, Vol. 22, pp. 562-564, 1973.
- [12] M.A. Md Zawawi, Advanced In<sub>0.8</sub>Ga<sub>0.2</sub>As/AlAs resonant tunneling diodes for applications in integrated mm-waves MMIC oscillators, Thesis

- (PhD), University of Manchester, Manchester, United Kingdom, 2015.
- [13] M. Bhattacharya and P. Mazumder, "Convergence Issues in Resonant Tunneling Diode Circuit Simulation," *Proceedings of the 13<sup>th</sup> International Conference on VLSI Design*, 2000.
- [14] A. Matiss, A. Poloczek, W. Brockerhoff, W. Prost, and F. Tegude, "Large-signal analysis and AC modeling of sub-micron resonant tunneling diodes," In: *Microwave Integrated Circuit Conference, 2007. EuMIC 2007. European*, pp.207-210, 2007.
- [15] S. F. Nafea and A. A. Dessouki, "An accurate large-signal SPICE model for Resonant Tunneling Diode," In: *Microelectronics (ICM)*, 2010, pp. 507-510.
- [16] Lai Chin Hoong and Shahrir R. Kasjoo, "Effect of Structural Parameters on Current-Voltage Properties of GaAs-based Resonant Tunneling Diodes Using Device Simulator," *International Journal of Nanoelectronics and Materials*, Volume 16 (Special Issue) December 2023.
- [17] X. Fang, B. Zhang, Y. H. Qin and Y. B. Wen, "Design of U-band Frequency Doubler Based on Schottky Diode MA4E1317,"Photonics & Electromagnetics Research

- Symposium (PIERS), Chengdu, China, 2024, pp. 1-4, 2024
- [18] Guo, C., Shang, X.B., Lancaster, M.J., Xu, J., Powell, J., Wang, H., Alderman, B., and Huggard, P.G.," A 135–150-GHz Frequency Tripler with Waveguide Filter Matching". IEEE Trans. Microwave Theory Tech. 66, 4608–4616, 2018.
- [19] Siles, J.V.; Cooper, K.; Lee, C.; Lin, R.; Chattopadhyay, G.; Mehdi, I. A Compact Room-Temperature 510–560 GHz Frequency Tripler with 30-mW Output Power. In Proceedings of the 15th European Radar Conference (EuRAD), Madrid, Spain, 2, pp. 333–336, 2018.
- [20] A. Sellai, H. Al-Hadhrami, S. Al-Harthy, M. Henini, "Resonant tunneling diode circuits using Pspice", Microelectronics Journal, Volume 34, Issues 5–8, 2003, pp. 741-745.
- [21] Z. Chen, H. Wang, A. Byron, H. Peter, B. Zhang, Y. Fan, "190 GHz high power input frequency doubler based on Schottky diodes and AlN substrate," IEICE Electronics Express, vol. 13, no.22, pp.1-12, 2016.
- [22] Zhang, B., Ji, D.F., Fang, D., Liang, S.X., Fan, Y., and Chen, X.D. "A Novel 220 GHz GaN Diode On-Chip Tripler with High Driven Power", IEEE Electron Device Letters, vol. 40, no. 5, pp. 780-783, 2019.